Calculation of ESR spectra and related Fokker–Planck forms by the use of the Lanczos algorithm[a)]

Giorgio Moro[b)] and Jack H. Freed

Department of Chemistry, Cornell University, Ithaca, New York 14853
(Received 24 October 1980; accepted 11 December 1980)

The applicability of the Lanczos algorithm in the general ESR (and NMR) line shape problem is investigated in detail. This algorithm is generalized to permit tridiagonalization of complex symmetric matrices characteristic of this problem. It is found to yield very accurate numerical solutions with *at least* order of magnitude reductions in computation time compared to previous methods. It is shown that this great efficiency is a function of the sparsity of the matrix structure in these problems as well as the efficiency of selecting an approximation to the optimal basis set for representing the line shape problem as distinct from actually solving for the eigenvalues. Furthermore, it is found to aid in the analysis of truncation to minimize the basis set (MTS), which becomes nontrivial in complex problems, although the efficiency of the method is not very strongly dependent upon the MTS. It is also found that typical Fokker–Planck equations arising from stochastic modeling of molecular dynamics have the property of being representable by complex-symmetric matrices that are very sparse, so calculation of associated correlation functions can be very effectively implemented by the Lanczos algorithm. It is pointed out that large problems leading to matrices of very large dimension can be efficiently handled by the Lanczos algorithm.

I. INTRODUCTION

The connection between ESR spectra and the dynamics of the rotational motion of the paramagnetic probe is well established, and it can be expressed by means of the relation[1]

$$I(\omega) = (1/\pi)\,\mathrm{Re}\,\{\langle v\,|[i(\omega\mathbf{1} - \mathfrak{L}) + \Gamma]^{-1}\,|v\rangle\}\,, \qquad (1)$$

where $I(\omega)$ is the intensity of the absorption as a function of the sweep frequency ω, $|v\rangle$ is the vector of the allowed spectral components, $\mathfrak{L}$ is the Liouville operator associated with the Hamiltonian of the magnetic interactions for the spin probe, and Γ is the (symmetrized) diffusion operator for the stochastic variables that modulate the magnetic interactions, i.e., the Euler angles that describe the orientation of the spin probe. The vectors and the operators are defined in the product space of the ESR transitions and the functions of the stochastic variables.

The theoretical simulation of ESR spectra is a powerful tool in extracting information about the dynamics of rotational motion. In fact the spectra in the so-called slow motional region are sensitive to the form of the diffusion operator Γ and, in principle, it is possible to distinguish between different models for the motion by comparison between experimental and theoretical spectra.[2] Therefore, future applications of ESR spectroscopy will be strongly dependent upon the efficiency of the algorithm for calculating simulated spectra. Recently there have been developments in the theory of molecular rotational motion in the liquid state that go beyond the usual hypothesis of Brownian motion.[3] As a matter of fact the utilization of these new models implies calculations with matrices that increase geometrically in dimension.

On the other hand there are a growing number of applications of the EPR technique, with corresponding simulation of spectra, to systems of physical or biological relevance with the purpose of deriving the relaxation time for the reorientational motion.[4a] In this field simple forms for the diffusion operator are utilized, thus the magnitude of the matrix is relatively small. But the use of a very compact algorithm that does not need a large core memory will allow the utilization of minicomputers directly connected to ESR spectrometers with considerable saving in time thus increasing the range of applications. Furthermore, we note that with the development of new NMR pulse techniques, it has been possible to obtain NMR line shapes in the slow motional region, which are also analyzed in terms of Eq. (1).[4b] In the future, one expects to see a growing number of applications requiring detailed spectral simulations.

The preferred way for obtaining the simulated spectrum from relation [Eq. (1)] is to diagonalize the complex symmetric matrix $\Gamma - i\mathfrak{L}$ and thereupon, from the eigenvalues and the transformed vector $|v\rangle$, to calculate the absorption or its derivative for each value of the frequency ω. In this scheme the usual procedure used is to transform the banded matrix into tridiagonal form by means of the algorithm developed by Rutishauser[5] (hereafter we shall call it the Rutishauser algorithm) followed by the application of the QR algorithm in order to derive the eigenvalues.[6] The tridiagonalization process imposes the limitations of this scheme from both the point of view of the time of calculation, since it is much slower than the following QR algorithm and the previous construction of the matrix, and the requirements of core memory, because storage of the matrix (in a banded form) is required. Moreover, in order to solve problems with large matrices one needs to consider a secondary storage such as a disk with considerable increase in calculation time for reading and writing between core memory and disk.

In recent years there has been an increasing interest in the Lanczos algorithm with a growing number of applications to different fields of research characterized by the large size of the matrices.[7] A related approach

[a)]Supported by NSF Grants DMR-77-17510, CHE 77-26996, and NIH Grant GM-25862-02.
[b)]Present address: Instituto di Chimica Fisica, Universita di Padova, Padova 35100, Italy.

 0021-9606/81/073757-17$01.00 © 1981 American Institute of Physics

has been applied by Alexander *et al.*[8] to ESR problems with emphasis on the study of the asymptotic structure of the ESR matrices for simple problems which can readily be handled by standard methods.

The purpose of this work is to extensively investigate the application of the Lanczos algorithm[9] in the calculation of ESR spectra as an alternative and preferable way in order to tridiagonalize the often large and complex matrices.[10]

The Lanczos method uses as intermediate results in the computation only the components of two vectors and it does not modify the original matrix. Therefore, it is convenient when the matrix is very sparse (and this is the case for ESR problems) so that only the elements different from zero are stored. Moreover, programs can be written so that the elements are generated when they are needed, which in our opinion is a very appealing way when the computer has an insufficient core memory. The substantial savings in execution time realized for our types of problems arises mainly from the sparsity of the matrices as well as the fact that the Lanczos algorithm may generally be employed in a number of iterative steps that are much less than the matrix dimension but still sufficient to accurately simulate the spectrum. This latter feature is partially related to the fact that the number of eigenvalues that make significant contributions to the spectrum is typically only a small fraction of the matrix dimension.

Both these considerations strongly support the use of the Lanczos algorithm from a computational point of view. We think there are other reasons that justify the use of this algorithm. One is connected to what we call the minimum truncation scheme (MTS): One desires a truncation scheme for the matrix $i\mathcal{L} - \Gamma$, which in itself is infinite, so that the dimension of the problem is reduced to a minimum, consistent with the spectrum remaining correct to a reasonable accuracy. In our opinion the solution of the truncation problem is as important as the algorithm for the diagonalization in order to minimize calculation time for a given problem. The Lanczos algorithm, together with some empirical rules, can give useful information about the MTS.

The Lanczos algorithm can be studied within the framework of what is called the theory of moments.[11,12] This generalization establishes a connection between such types of mathematical formalism as continued fractions and Padé determinants,[13] that in our opinion, allows us to consider the calculation of ESR spectra in a more general way. On the one hand we consider this generalization very important, because it justifies the use of the Lanczos algorithm beyond a mere computational device, while, on the other hand we can apply some results of the theory of moments to our problem in at least a qualitative way. The theory of moments and the Lanczos algorithm have been well studied for symmetrical real operators, but to our knowledge there is very little work on complex symmetric problems such as Eq. (1).

The range of potential applications that involve complex symmetric operators is wide and goes beyond the simulation of ESR spectra. In particular, the general class of Fokker–Planck equations, such as those recently developed[3] are, in general, represented by complex symmetric operators, due to the existence of both inertial or drift terms and damping terms. The calculation of time correlation functions (or more precisely their Fourier–Laplace transforms) is also found to proceed from expressions like Eq. (1), and, furthermore, they are found to have the characteristics of: (1) sparse bounded matrix structure, and (2) only a few contributing eigenvalues.[3b] This to our mind, guarantees the utility of the Lanczos algorithm for complex symmetric matrices for this important class of problems.

We give in Sec. II a summary of the Lanczos algorithm that is appropriate for the solution of problems of the type described by Eq. (1), while in Sec. III the computational details relating to the convergence and the efficiency of the method are given. In Sec. IV, we discuss the important matter of the minimum truncation scheme. The application of the Lanczos algorithm to Fokker–Planck equations in the study of molecular dynamics is outlined in Sec. V with reference to a simple example. Our conclusions appear in Sec. VI.

II. THE LANCZOS ALGORITHM

The Lanczos algorithm[9,10] can be seen as an application of the more general theory of approximation of operators known as the method of moments in Hilbert space.[11,12] In that method the n-dimensional approximation $\mathbf{A}_n$ of an operator $\mathbf{A}$ for a fixed starting vector $|z\rangle$ is given by the relation

$$\mathbf{A}_n = \mathbf{P}_n \mathbf{A} \mathbf{P}_n , \tag{2}$$

where $\mathbf{P}_n$ is the projection in the subspace defined by the vectors generated by operator $\mathbf{A}^{(k-1)}$ acting on the starting vector $|z\rangle$ with $k=1$ to n (i.e., the vectors $|z_k\rangle = \mathbf{A}^{(k-1)}|z\rangle$). If the operator $\mathbf{A}$ is symmetric or self-adjoint, the method of moments is equivalent to the Lanczos algorithm, which generates a tridiagonal form for $\mathbf{A}_n$ by means of developing a proper representation of the n-dimensional subspace. This representation, which we label as $|k\rangle$, is produced from the $|z_k\rangle$ by a Schmidt orthonormalization process. This algorithm clearly yields a procedure for iteratively generating the new basis set $|k\rangle$.

Let us first consider the algorithm in a real Hermitian space. Then the first new basis element is given by the starting vector properly normalized

$$|1\rangle = \|z\|^{-1}|z\rangle \tag{3}$$

and the kth new basis element $|k\rangle$ for $1 < k \leq n$ is defined as

$$\beta_k |k\rangle = (1 - \mathbf{P}_{k-1})\mathbf{A}|k-1\rangle , \tag{4}$$

where the coefficient β_k is uniquely defined by the normalization condition for $|k\rangle$ and the projection operator $\mathbf{P}_k$ can be written as

$$\mathbf{P}_k = \sum_{j=1}^{k} |j\rangle\langle j| . \tag{5}$$

From definition (4), the following properties are immediately derived:

(i) $\mathbf{A}_n$ is symmetric.

(ii) $\mathbf{A}_n$ is tridiagonal (i.e., $\mathbf{A}_n \equiv \mathbf{T}_n$). In fact, considering the scalar product $\langle j|k\rangle$ for $j > k$ we have

$$0 = \langle j|k\rangle = \beta_k^{-1}\langle j|(1-\mathbf{P}_{k-1})\mathbf{A}|k-1\rangle = \beta_k^{-1}\langle j|\mathbf{A}|k-1\rangle .$$

(iii) The coefficients β_k define the off-diagonal elements of $\mathbf{T}_n$:

$$\beta_k = \langle k|(1-\mathbf{P}_{k-1})\mathbf{A}|k-1\rangle = \langle k|\mathbf{A}|k-1\rangle . \tag{6}$$

Therefore, the recursive relation (4) can be written more explicitly with the use of Eq. (5) as

$$\beta_k|k\rangle = (\mathbf{A}-\alpha_{k-1}1)|k-1\rangle - \beta_{k-1}|k-2\rangle , \tag{7}$$

where α_k is the kth diagonal element of $\mathbf{T}_n$.

The Lanczos algorithm can be applied to complex Hermitian spaces in two different ways according to the property of symmetry of the matrix. The previous definitions are immediately extended to a self-adjoint matrix yielding a self-adjoint tridiagonal matrix by means of the recursive relation

$$\beta_k|k\rangle = (\mathbf{A}-\alpha_{k-1}1)|k-1\rangle - \beta_{k-1}^*|k-2\rangle . \tag{8}$$

Instead, for complex symmetric matrices such as $\mathbf{\Gamma} - i\mathfrak{L}$ in the relation (1), the Schmidt orthonormalization process does not generate a tridiagonal matrix and it destroys the symmetry of the matrix. The Lanczos algorithm can be extended to this situation if the new basis set satisfies the relation

$$\sum_j \langle x_j|m\rangle\langle x_j|l\rangle = \delta_{ml} , \tag{9}$$

where the summation is taken over all the elements $|x_j\rangle$ of the starting basis set in which $\mathbf{A}$ is symmetric. This implies a pseudo-Schmidt orthonormalization process in which the bra vectors for definition (5) of the projectors are

$$\langle k| = \sum_j \langle x_j|k\rangle\langle x_j| . \tag{10}$$

Or, equivalently, the scalar product is defined without the complex conjugate of the components of the bra vectors and this assures the validity of Eqs. (3)–(7) in a space that is no longer metric. Note that the starting vector $|z\rangle$ must be normalized accordingly, that is, its pseudonorm is defined as

$$\|z\|^2 = \sum_j \langle x_j|z\rangle^2 , \tag{11}$$

that generally is a complex quantity.

In order to solve Eq. (1), this version of the Lanczos algorithm can be applied to $\mathbf{A} = \mathbf{\Gamma} - i\mathfrak{L}$, with $|v\rangle$ of Eq. (1) as starting vector by using Eq. (7). The following relation is obtained for the spectral function in the n-dimensional approximation for $\mathbf{A}$:

$$I_n(\omega) = (1/\pi)\,\mathrm{Re}\{\langle 1|[(1/T_2^0 + i\omega)\mathbf{1} + \mathbf{T}_n]^{-1}|1\rangle\} , \tag{12}$$

where $|1\rangle$ is the normalized starting vector in the new basis set [cf. Eq. (3)]. [The derivation of Eq. (12) is given in Appendix A.] At this point, the version of the QR algorithm for a complex symmetric matrix[6] can be used to generate the eigenvalues λ_j of T_n and the components c_j of $|1\rangle$ with respect to the eigenvectors $|y_j\rangle$, so that the absorption, or the (experimentally more relevant) derivative, is calculated as a function of the sweep frequency

$$I_n(\omega) = \frac{1}{\pi}\,\mathrm{Re}\left(\sum_{j=1}^{n} \frac{c_j^2}{\lambda_j + 1/T_2^0 + i\omega}\right) , \tag{13a}$$

$$I_n'(\omega) = \frac{dI_n(\omega)}{d\omega} = \frac{1}{\pi}\,\mathrm{Im}\left[\sum_{j=1}^{n} \frac{c_j^2}{(\lambda_j + 1/T_2^0 + i\omega)^2}\right] . \tag{13b}$$

As an alternative way the spectrum can be simulated directly from the tridiagonal matrix by means of a continued fraction formalism:

$$I_n(\omega) = -(1/\pi)\mathrm{Re}(f_1) , \tag{14a}$$

$$I_n'(\omega) = \frac{1}{\pi}\,\mathrm{Re}\left(\sum_{j=1}^{n}\prod_{l=1}^{j}\beta_l^2 f_l^2\right) , \tag{14b}$$

where f_j stands for the continued fraction[25]

$$f_j = \cfrac{-\beta_j^2}{(1/T_2^0 + i\omega + \alpha_j) + \cfrac{-\beta_{j+1}^2}{(1/T_2^0 + i\omega + \alpha_{j+1}) + \cdots \cfrac{-\beta_n^2}{+(1/T_2^0 + i\omega + \alpha_n)}}} , \tag{14c}$$

with $\beta_1 \equiv -1$. In Appendix A the derivation of Eqs. (14a) and (14b) are sketched.

We mention that the continued fraction representation of the spectral function [Eq. (14a)] can be seen in the context of the Padé approximants.[13] In fact, applying the arguments of Ref. 12, the spectral function can be related to the $[n+1, n]$ Padé approximant constructed with the coefficients a_j of the power-series development $\langle v|(1+w\mathbf{A})^{-1}|v\rangle = \sum_j a_j w^j$, where $w = 1/(1/T_2^0 + i\omega)$. From this point of view, the Lanczos algorithm constitutes a method for generating the proper function [i.e., the continued fraction (14a)], that converges in the region around $1/w = 0$ for $\mathrm{Re}(w) > 0$.

The connection between the Lanczos algorithm and the method of moments emphasizes how this algorithm produces subspaces that progressively approximate the given operator. The rapidity of convergence of the spectral function with increases in dimension of these subspaces determines the efficiency of the algorithm in the calculation of ESR spectra. The problem of the convergence can be seen in the full (i.e., infinite) space in which the operator $\mathbf{\Gamma} + i\mathfrak{L}$ is defined. One would like to have a general theorem that guarantees in all generality the convergence of the spectral function. To our knowledge in the framework of the moment method there are only theorems for bounded or self-adjoint operators[11,12] while our operator is complex symmetric and, in general, unbounded because of the diffusion operator $\mathbf{\Gamma}$. On the other hand, this type of convergence is equivalent to the statement that the spectral function [Eq. (1)] exists, and this can be taken as an implicit and physically justified assumption in the theory of ESR spectra (and related Fokker–Planck forms, cf. Sec. V).

If the starting vector has a finite number of components (as is the case for isotropic media, see Appendix B) the calculation of ESR spectra by means of the Lanczos algorithm can be done without introducing any truncation in the matrix associated to $\mathbf{\Gamma} + i\mathfrak{L}$ because this matrix has a band structure and, therefore, the

calculation of $\mathbf{T}_n$ for a fixed n involves only a finite submatrix. However in practical applications, it is always convenient to fix the truncation independently of the number of steps in order to reduce computation time. Then the convergence of the spectral function is assured [the approximated form of Eq. (2) of the operator coincides with the truncated form of the operator when $n=N$, N being the dimension of its matrix representation]. While the rate of convergence with increasing number of steps is of major importance for practical applications, there is to our knowledge no theoretical analysis of the convergence rate that is applicable for our type of matrices. On the other hand we find that, in general, the spectral function reaches (to a specified reasonable accuracy) its convergent form with a number of steps considerably less than the dimension of the matrix. We think that the concept of the optimal reduced space is useful in explaining these results. We define the optimal reduced space as the subspace with the least dimension and with a representation of the matrix that generates a spectrum correct to within a fixed accuracy with respect to the full solution. If one thinks of the relation (13a) in terms of the eigenvalues of the full space, this subspace is related to the eigenvectors characterized by a weight $|c_j^2|$ greater than some fixed value. {Note that in Eq. (13a) the height, as distinct from the intensity, of the jth component is inversely proportional to $\mathrm{Re}(\lambda_j)$ while for Eq. (13b) it is inversely proportional to $[\mathrm{Re}(\lambda_j)]^2$. Thus very broad components may contribute less significantly to the spectrum than this criterion would imply.} The Lanczos algorithm can be interpreted as constructing subspaces that progressively approximate that optimal reduced space. Consequently, the choice of $|v\rangle$ as starting vector is dictated not only by the economy of the algorithm in order to avoid the computation of $|v\rangle$ with respect to the new basis set, but also by the consideration that the vector $|v\rangle$ through its projections c_j selects the optimal reduced space.

In practical computer applications the main weakness of the Lanczos algorithm is the loss of orthogonality between the calculated new basis set as a consequence of the round-off error.[9(b),14,15] As a consequence the method continues indefinitely beyond the dimension of the matrix and it produces spurious eigenvalues. In a true eigenvalue problem this limits the application of the Lanczos algorithm in its original form, because of the identification problem for the eigenvalues, but the use of the algorithm in a more sophisticated form could be employed to overcome the loss of orthogonality.[9(b)] For our sort of problems the original form of the Lanczos algorithm is adequate because:

(i) We are not strictly concerned with the eigenvalues. In fact, by means of Eqs. (14a) and (14c), the spectrum can be calculated directly from the tridiagonal matrix. Therefore any approximate form of $\mathbf{T}_n$ is adequate, independent of the effect of the loss of orthogonality, if it reproduces the spectral function well. In this context it is still useful to analyze the eigenvalues associated with $\mathbf{T}_n$ in order to understand how the Lanczos algorithm functions in our type of problems.

(ii) It is well known that the loss of orthogonality is important only when the number of steps approaches the dimension of the space.[14] Generally we do not need to reach such situations, since sufficient convergence is reached for $n \ll N$.

III. COMPUTER RESULTS

A. General considerations

Since the Lanczos algorithm is defined by the same recursive equation (7) for both complex and real symmetric matrices, we used a standard form of that algorithm for real matrices,[16] modified only for the complex arithmetic and in which the storage of only two vectors is needed. All the calculations were made with a PDP 11/34 minicomputer (64 kbytes of program memory) with a data memory of 196 kbytes. The required matrix elements were stored in data memory while the vectors were stored in program memory. With this type of organization the Lanczos algorithm allows us to solve ESR problems related to matrices with a maximum dimension of 870, but this covers almost the whole range of conventional spectral simulations. Once the tridiagonal matrix $\mathbf{T}_n$ is obtained, the spectrum is calculated by means of the continued fraction method defined by Eqs. (14a)–(14c). In the case where one needs the eigenvalues of $\mathbf{T}_n$, the standard QR algorithm for complex symmetric matrices[6] can be used. A previous program written for the PDP 11/34, that calculates by a form of the Rutishauser algorithm followed by the QR algorithm the ESR spectrum for a nitroxide probe (nuclear spin equal to one) or for only the g tensor, was utilized to obtain the correct eigenvalues and to compare the respective calculation times for the two algorithms. The particular form of the Rutishauser algorithm is one we developed for a minicomputer with disk storage of the matrix elements,[17] in which the sequence of equations is modified with respect to the standard form of the algorithm[5] for complex symmetric matrices,[6] in order to have maximum efficiency in communication between core memory and disk. In that form of the algorithm, the limit on the size of the matrix is given by the available space in the disk, but for a practical point of view, its utilization is limited by the execution time (e.g., a typical ESR problem with a matrix dimension of 600 requires about one day).

We assume in our analysis a Smoluchowski diffusion equation for the rotational motion. In Appendix B, the derivation of the matrix elements of $(\Gamma - i\mathcal{L})$ together with the specific conditions on the magnetic interactions, are described.

Since the Lanczos algorithm is an iterative procedure that utilizes the specific form of the matrix to construct successive approximations, its behavior, and therefore its efficiency, depends strongly on the type of problem to which it is applied. As a consequence, it cannot be used as a pure computational tool independent of the particular structure of the problem. On the other hand, the performance of the Rutishauser algorithm, once the dimension and the bandwidth are chosen, is not specifically related to the nature of the problem. In the following part the computer results for some typical situations, covering the usual applications of ESR spectroscopy in

TABLE I. Magnetic, diffusion, and truncation parameters.[a]

	g_{xx}	g_{yy}	g_{zz}	B_0[b]	I	A_{xx}[b]	A_{yy}[b]	A_{zz}[b]	$D_\perp$[c]	$D_\parallel$[c]	λ	L_{max}	K_{max}	N	n_s[d]
I[e]	2.007	1.973	2.02	3300	···	···	···	···	2.5×10^6	6.5×10^6	0	16	12	42	16
II	2.007	1.973	2.02	3300	···	···	···	···	2.5×10^6	6.5×10^6	0	24	18	85	19
III	2.007	1.973	2.02	3300	···	···	···	···	2.5×10^6	7.5×10^8	0	16	12	42	34
IV	1.991	1.989	2.02	3300	···	···	···	···	2.5×10^6	6.5×10^6	0	16	12	42	10
V	2.007	1.973	2.02	3300	···	···	···	···	2.5×10^6	6.5×10^6	10	16	12	42	9
VI[e]	2.008	2.008	2.002	3300	1	5	5	34	10^6	···	0	18	0	57	45
VII	2.008	2.008	2.002	3300	1	5	5	34	10^6	···	0	30	0	93	56
VIII	2.008	2.008	2.002	3300	1	0.5	0.5	3.4	10^6	···	0	18	0	57	26
IX	2.008	2.008	2.002	3300	1	5	5	34	10^6	···	10	18	0	57	21
X[e]	2.005	2.009	2.002	3300	1	2	19	32	7×10^5	7×10^5	0	16	12	330	63

[a] See Appendix B for the meaning of the symbols.
[b] In G.
[c] In sec^{-1}.
[d] Sufficient number of steps according to relation (16).
[e] In these calculations L_{max} and K_{max} constitute the MTS with respect to the accuracy of 10^{-4}.

the slow motional region, are analyzed with particular emphasis on the relation between the behavior of the Lanczos algorithm and the features of the problem. This can be done in only a partially quantitative manner, and we will also use more qualitative concepts, like that of the optimal reduced space (cf. Sec. II).

In order to analyze the convergence problem for the Lanczos algorithm, we define the error in the spectrum as a function of the number of steps for fixed diffusion, magnetic and truncation parameters (i.e., size of the matrix), as

$$\Delta_n = \int_{-\infty}^{+\infty} |I_R(\omega) - I_n(\omega)|\, d\omega \,, \tag{15}$$

where $I_R(\omega)$ is the exact spectrum (i.e., the normalized spectrum in absorption obtained from the Rutishauser algorithm), and $I_n(\omega)$ is the spectrum obtained from the Lanczos algorithm applied for n steps. Note that both $I_R(\omega)$ and $I_n(\omega)$ are normalized:

$$\int_{-\infty}^{+\infty} I_R(\omega)\, d\omega = \int_{-\infty}^{+\infty} I_n(\omega)\, d\omega = 1 \,.$$

In order to illustrate concisely the convergence to the correct spectrum, $E_n = -\log_{10}(\Delta_n)$ is plotted against n in Figs. 3 and 4. The diffusion, magnetic, and truncation parameters used in the calculations are given in Table I. Since our purpose is to use the Lanczos algorithm with the least number of steps consistent with obtaining a correct spectrum, we define the sufficient number of steps n_s as the minimum n satisfying the condition

$$\Delta_n \leq 10^{-4} \,. \tag{16}$$

This corresponds to the condition that there is no visible difference between $I_R(\omega)$ and $I_n(\omega)$, i.e., accuracy better than can be achieved experimentally. We note that the problem of convergence has two aspects: (1) the required size of the matrix N (which is independent of the specific algorithm for the diagonalization), and (2) for fixed N, the value of n_s for the Lanczos algorithm. The former (i.e., the truncation of the matrix) is discussed in the following section, while here we specifically consider the second aspect. Thus we start with specific cases in which aspect (1) has already been resolved; i.e., we already have what we call the minimum truncation scheme (MTS) for the particular set of values of diffusion and magnetic parameters. This implies that we have K_{max} and L_{max} (where the indices K and L are defined in Appendix B) leading to the smallest value of N consistent with the spectrum being correct within an accuracy of 10^{-4} (see Sec. IV) We have, for purposes of our tests, explicitly determined these values. (It is immaterial whether the Rutishauser or the Lanczos algorithm is used for this purpose.)

B. Examples

We now discuss in detail the results for one case (viz., Table I, case I) which displays the characteristic behavior of the Lanczos algorithm seen in much more complicated cases, even though it is a simple calculation of the slow motional spectrum for an anisotropic g tensor, (e.g., Fig. 1). In Table II the eigenvalues and

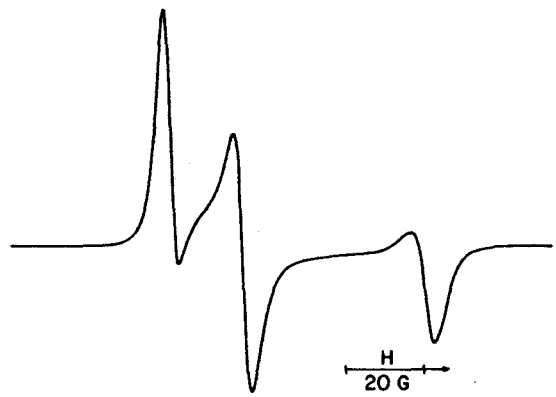

FIG. 1. Derivative spectrum for a nonaxial g tensor (see Table I, case I, for the magnetic, diffusion and truncation parameters).

TABLE II. Eigenvalues and components from the Rutishauser algorithm applied to calculation I (see Table I).

	Eigenvalues (λ_j)		Components (c_j^2)	
j	Real	Imaginary	Real	Imaginary
1	4.2533	−9.6223	0.16413	0.64141×10^{-3}
2	5.3351	38.981	0.82995×10^{-1}	0.87541×10^{-1}
3	3.4612	−29.416	0.83186×10^{-1}	-0.86460×10^{-1}
4	8.7559	−14.823	0.84263×10^{-1}	0.40377×10^{-2}
5	15.937	3.0708	0.83192×10^{-1}	-0.20804×10^{-2}
6	8.4422	−24.394	0.39234×10^{-1}	-0.65563×10^{-1}
7	17.252	−8.9660	0.68361×10^{-1}	0.21037×10^{-1}
8	16.889	26.082	0.39064×10^{-1}	0.47402×10^{-1}
9	13.911	29.544	0.43119×10^{-1}	0.43451×10^{-1}
10	12.747	−20.023	0.50359×10^{-1}	-0.32527×10^{-1}
11	17.668	4.5846	0.55391×10^{-1}	0.16298×10^{-1}
12	17.763	18.025	0.54082×10^{-1}	0.16208×10^{-1}
13	23.683	14.814	0.42033×10^{-1}	0.38758×10^{-2}
14	21.822	−7.3724	0.11539×10^{-1}	-0.38167×10^{-1}
15	11.874	−19.653	0.33228×10^{-1}	-0.18009×10^{-1}
16	20.669	−2.9274	0.35822×10^{-1}	-0.13673×10^{-2}
17	24.551	16.864	0.79936×10^{-2}	0.18927×10^{-1}
18	25.132	6.6072	0.20213×10^{-1}	-0.22767×10^{-2}
19	19.789	−14.854	0.50900×10^{-3}	-0.17555×10^{-1}
20	16.230	−19.713	-0.30917×10^{-2}	0.20757×10^{-2}
21	27.335	−5.0499	-0.52585×10^{-3}	0.33323×10^{-2}
22	31.136	8.1608	0.22303×10^{-2}	-0.13070×10^{-2}
23	29.027	−8.2156	0.15157×10^{-2}	0.11256×10^{-2}
24	26.828	29.176	0.79231×10^{-3}	-0.38072×10^{-4}
25	25.397	−19.875	0.45374×10^{-3}	-0.11742×10^{-3}
26	35.825	−0.46477	0.49027×10^{-5}	-0.33185×10^{-3}
27	36.899	19.967	-0.34792×10^{-4}	-0.10306×10^{-3}
28	41.270	23.188	-0.61962×10^{-4}	0.85753×10^{-4}
29	40.404	7.2359	-0.41851×10^{-4}	-0.90946×10^{-4}
30	31.230	−19.464	0.82025×10^{-4}	-0.15358×10^{-5}
31	23.109	−19.707	-0.10875×10^{-4}	-0.31637×10^{-4}
32	31.298	−21.328	-0.98443×10^{-5}	-0.11906×10^{-4}
33	46.463	4.1298	-0.12138×10^{-4}	0.50214×10^{-5}
34	37.457	−17.008	0.84510×10^{-5}	-0.52566×10^{-5}
35	49.782	17.718	0.24899×10^{-6}	0.64558×10^{-5}
36	35.472	−17.538	-0.48422×10^{-5}	-0.20440×10^{-5}
37	44.099	9.4065	-0.51339×10^{-5}	0.27728×10^{-8}
38	41.517	−4.2402	-0.12162×10^{-5}	-0.21922×10^{-5}
39	45.309	−12.324	-0.76693×10^{-6}	-0.68177×10^{-6}
40	54.155	−6.7230	-0.37865×10^{-7}	0.10999×10^{-6}
41	52.981	5.6905	0.27077×10^{-7}	0.35344×10^{-7}
42	64.565	0.85538	0.27954×10^{-8}	-0.72428×10^{-8}

the square of the components from the Rutishauser algorithm are listed. The sufficient number of steps n_s with the Lanczos algorithm is 16 (cf. Fig. 3). The eigenvalues and the square of the components calculated by means of the QR algorithm applied to the tridiagonal matrix generated by the Lanczos algorithm in 16 steps, are listed in Table III and the distribution of the eigenvalues obtained from the two algorithms is represented in Fig. 2.

Based on these (and many other) results we make the following observations:

(i) Given the criterion of Eq. (16), then we need only consider the set of eigenvectors $|y_j\rangle$ such that $|c_j^2| \geq 10^{-4}$, where $c_j \equiv \langle y_j | v \rangle$. Then we find that the Rutishauser algorithm needs 28 eigenvalues to reproduce the spectrum, while the Lanczos algorithm reduces the problem to a subspace of dimension 16.

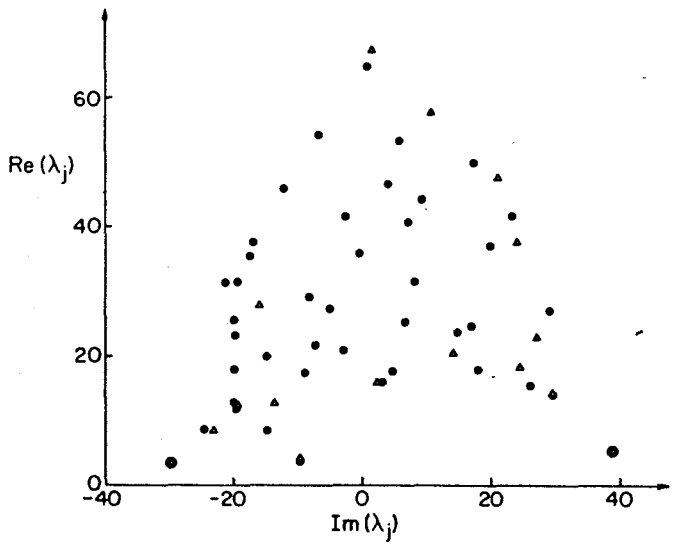

FIG. 2. Distribution of the eigenvalues for calculation I (see Table I). The units are in G. The x axis and y axis represent, respectively, the imaginary and real parts of the eigenvalues. △: eigenvalues from the Lanczos algorithm listed in Table III; ●: eigenvalues from the Rutishauser algorithm listed in Table II. (Note that for the three λ_j with smallest Re(λ_j), the two algorithms give virtually identical results.

(ii) Only 7 eigenvalues from Table III find a correspondence with the "exact" eigenvalues. There is generally less agreement between the eigenvalues in the two methods as the real parts of the eigenvalues increase in magnitude.

(iii) If we assume that each eigenvalue and its corresponding component c_j obtained from the Lanczos algorithm approximates the analogous "exact" quantities, only the sets nos. 4 and 5 in Table III have a sufficient accuracy to predict with an error less than 10^{-4} the lineshape described by the corresponding "exact" set (nos. 2 and 3 in Table II).

The Lanczos algorithm approximates the spectrum surprisingly well in spite of a rather low accuracy for

TABLE III. Eigenvalues and components from the Lanczos algorithm with 16 steps in calculation I (see Table I).

	Eigenvalues (λ_j)		Components (c_j^2)	
j	Real	Imaginary	Real	Imaginary
1	12.776	−13.415	0.23643	0.65377×10^{-1}
2	15.886	2.4657	0.16654	-0.15140×10^{-1}
3	4.1561	−9.5836	0.15142	0.31806×10^{-2}
4	5.3351	38.981	0.82995×10^{-1}	0.87541×10^{-1}
5	3.4612	−29.416	0.83177×10^{-1}	-0.86461×10^{-1}
6	13.468	−19.312	0.29865×10^{-1}	−0.10649
7	20.243	14.329	0.10418	0.57283×10^{-2}
8	18.127	24.607	0.60629×10^{-1}	0.73134×10^{-1}
9	8.3990	−24.409	0.40133×10^{-1}	-0.63006×10^{-1}
10	13.965	29.471	0.46912×10^{-1}	0.47215×10^{-1}
11	22.803	27.223	-0.22153×10^{-2}	-0.11259×10^{-1}
12	37.420	23.244	0.20855×10^{-3}	0.24882×10^{-3}
13	27.695	−15.726	-0.28168×10^{-3}	-0.61059×10^{-4}
14	47.104	21.151	0.79661×10^{-5}	-0.11588×10^{-4}
15	57.347	10.920	0.16972×10^{-6}	-0.21962×10^{-7}
16	67.019	1.5835	-0.61199×10^{-9}	-0.15893×10^{-8}

the eigenvalues and their components. One way to have some insight, at least partially, into this behavior is to look at the results in terms of an approximation of clusters of eigenvalues instead of single eigenvalues. If we take as an example the eigenvalue no. 2 in Table III, which can be related to the exact eigenvalue no. 5 in Table II, then we find that $\mathrm{Re}(c_j^2)$ differs by a quantity of the order of 0.08. Instead, if we think of that eigenvalue as an approximation of the ensemble of the "exact" eigenvalues nos. 5, 11, and 16 of Table II, the sum of the $\mathrm{Re}(c_j^2)$ terms differ from the Lanczos value by a quantity of the order of 0.01. This organization in clusters is directly suggested by Fig. 2.

The concept of cluster is of course very qualitative, since its exact formulation is not possible. Moreover, the eigenvalues obtained from the Lanczos algorithm cannot be considered independent from one another in the evaluation of their effect on the spectrum. The unique way to characterize these results in all generality is to state that the Lanczos algorithm produces an approximation of the optimal reduced space required to represent spectral function *instead of* accurately reproducing the eigenvalues. In this context the interpretation in terms of clusters is only a partial and qualitative explanation of this general behavior.

There is no other method that gives the optimal reduced space, and the exact solution of the eigenvalue problem determines only an upper limit for its dimension, i.e., the number of eigenvalues with weight (i.e., $|c_j^2|$) greater than 10^{-4}. As a consequence, it is not possible to evaluate exactly how the Lanczos algorithm approximates the optimal reduced space; only some indications can be given comparing that upper limit with the actual number of steps needed (27 against 16 in the previous example). On the other hand, the results in Table III show that the Lanczos algorithm produces only an approximation to the optimal reduced space. In fact, the last three eigenvalues have a weight less than 10^{-4} and they are not necessary to reproduce the spectrum with the condition equation (16).

We may relate the fact that the Lanczos algorithm only approximates the optimal reduced space to what we call the extreme eigenvalue effect. It is known that the method of moments tends to seek out the eigenvalues of larger magnitude.[11,18] If the starting vector $|z\rangle$ is expanded in terms of the eigenvectors $|y_j\rangle$ of the exact operator $\mathbf{A}$ ($\mathbf{A}|y_j\rangle = \lambda_j|y_j\rangle$), i.e.,

$$|z\rangle = \sum_j a_j |y_j\rangle , \tag{17}$$

then the kth vector generated by the method of moments can be written as

$$|z_k\rangle = \mathbf{A}^{k-1}|z\rangle = \sum_j a_j \lambda_j^{k-1} |y_j\rangle . \tag{18}$$

Therefore by increasing the order of approximation for $\mathbf{A}$ (i.e., by increasing k) the method of moments tends to include in the subspace defined by P_n in Eq. (2), the eigenvectors with larger λ_j. This extreme eigenvalue effect will be stronger the larger the magnitude of the coefficients a_j in Eq. (17) for the larger eigenvalues relative to those for the smaller ones. The same effect is generated by the Lanczos algorithm, since it is a particular case of the method of moments.

In our problems, the extreme eigenvalue effect can be further analyzed in terms of the particular structure of the matrix. The Liouville operator has matrix elements whose orders of magnitude are independent of the value of the K and L indices, and these matrix elements quickly reach a constant (asymptotic) form determined by the asymptotic values of the relevant $3j$ symbols.[19] On the other hand, the isotropic part of $\mathbf{\Gamma}$ yields only diagonal matrix elements that increase with the squares of the indices L and K. In calculations for isotropic systems (i.e., when $\lambda = 0$) like that previously described, we can approximately subdivide into two parts the basis set in which $\mathbf{\Gamma} - i\mathbf{\mathcal{L}}$ is represented before the application of the Lanczos algorithm:

(i) The subset that is strongly mixed into the solution of the eigenvalue problem: This subset is characterized by off-diagonal matrix elements with the same order of magnitude as the diagonal ones. Thus it is defined by those elements of the basis set with small values of the indices K and L relative to $K_{\max}$ and $L_{\max}$. This subset leads to eigenvalues characterized by an imaginary part that reflects the line position of the Lorentzians in a rigid limit spectrum, and a (relatively) small real part that determines their broadening.

(ii) The subset characterized by large diagonal elements with respect to the off diagonal ones: This subset is defined by the basis elements with K and L indices close to $K_{\max}$ and $L_{\max}$, respectively, and they have only a perturbational effect on the eigenvalues associated with the previous subset. The associated eigenvectors are well approximated by the eigenvectors of the diffusion operator [i.e., the Wigner rotation matrices $D^L_{KM}(\Omega)$] and the eigenvalues have a large real part.

Since the starting vector typically belongs to the first subset (e.g., for isotropic media it has nonzero components only for $L = 0$, see Appendix B), only the eigenvectors associated with this subset give a relevant contribution to the spectrum. But, as a consequence of the extreme eigenvalue effect, the Lanczos algorithm tends to insert also the eigenvalues related to the second subset, since they have the largest numerical value. In this way, we explain the appearance of the last three eigenvalues in Table III. On the other hand, the extreme eigenvalue effect only partially reduces the efficiency of the Lanczos algorithm (e.g., these three eigenvalues vs a total number of 16) because the coefficients a_j in Eq. (17) for subset (ii) have only small values.

Therefore, we can state that the combination of the extreme eigenvalue effect and the particular structure of the matrix associated with the Smoluchowski equation generates a departure from ideal behavior of the Lanczos algorithm (i.e., the optimal reduced space). This constitutes a negative feature of the application of the Lanczos algorithm to ESR problems, but it is inherent in the method and the previous results show how, in spite of this, the algorithm allows us to approximate the matrix in a subspace with dimension much smaller than

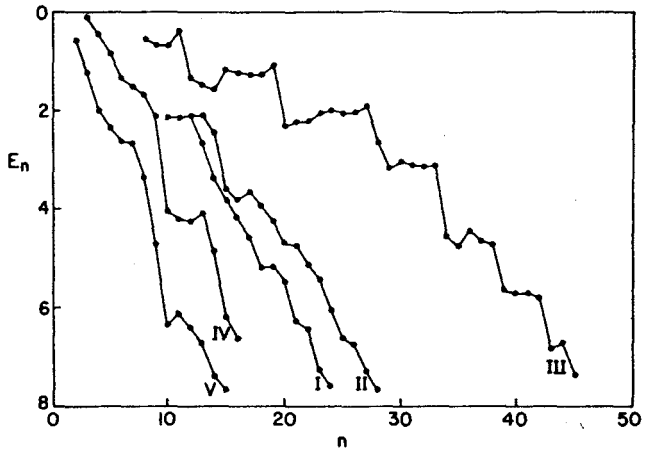

FIG. 3. Behavior of the logarithm of the error: $E_n = -\mathrm{Log}_{10}(\Delta_n)$ [Δ_n is defined in Eq. (15)] as a function of the number of steps n in the Lanczos algorithm. (See Table I for the magnetic, diffusion, and truncation parameters.)

the initial dimension of the matrix.

We now consider other examples which illustrate aspects of the convergence. Calculation II differs from calculation I only with respect to the truncation parameters K_{max} and L_{max}. Figure 3 shows how the increase in size of the matrix slows down convergence in the Lanczos algorithm. This can easily be explained in terms of the extreme eigenvalue effect. In fact, in this problem the increase of K_{max} and L_{max} is equivalent to enlarging the subset of type (ii) by inserting new basis elements that lead to eigenvalues numerically larger than in the calculation I. However, the effect is really quite small. Thus n_s only increases from 16 to 19 steps while the dimension of the matrix is more than doubled. This result illustrates one of the advantages in the use of the Lanczos algorithm. Since there is no exact criterion for the truncation (see Sec. IV), in routine calculations, the matrices are often truncated with larger dimension than strictly necessary. Thus ideal behavior of the Lanczos algorithm, from the point of view of computer effort, would be an invariant n_s with increasing dimension of the matrix. We found from the computer calculations that for most of the cases (e.g., the previous one) the performance of the Lanczos algorithm is close to ideal behavior.

In order to show how the extreme eigenvalue effect is specifically related to the structure of our matrices, in calculation III, the anisotropy of the motion (i.e., $D_\parallel/D_\perp$) is increased with respect to calculation I, but keeping $D_\perp$ and all the remaining parameters the same, while in calculation IV the degree of nonaxiality of the g tensor [i.e., $F_g^{(2,2)}$] is decreased, but with the diffusion and truncation parameters remaining the same. In both cases the size of the subset (i) is decreased with respect to calculation I, but in two different ways: increasing the diagonal matrix elements of the diffusion operator for $K \neq 0$ in calculation III and decreasing the off-diagonal matrix elements that connect basis elements with different K index in calculation IV (in both situations a K_{max} equal to 4 would be sufficient to reproduce the spectrum within an accuracy of 10^{-4}). We find that the extreme eigenvalue effect contributes much more in calculation III than in calculation IV. In fact, Fig. 3 shows that the convergence in calculation III is much slower not only than that in calculation IV, but also with respect to calculation I. We mention that a K_{max} close to 4 would reduce considerably the extreme eigenvalue effect. The departure from ideal behavior (i.e., the minimum optimal basis set) by the Lanczos algorithm, becomes more serious as we approach limiting cases like large anisotropy of the motion. However, in these cases good truncation of the matrix reduces the dimension of the problem thus partially compensating for the relatively poorer efficiency of the algorithm.

Calculation V includes a strong potential ($\lambda = 10$) corresponding to an order parameter $\overline{D_{00}^2}$ equal to 0.896. Since the diffusion operator is no longer diagonal in the starting representation of the matrix, it is not possible to apply the previous analysis of the contribution of the initial basis set to the spectrum. Instead, it is more useful to think in terms of the eigenvectors of the Smoluchowski operator Γ as the initial basis set. For this large value of λ, the asymptotic solution of the diffusion operator[10b),20] constitutes a good solution. The equation for the eigenvalues of Γ is more complicated than in the isotropic phase, but the main effect scales according to λ which is large. As a consequence, the basis vectors strongly coupled by the Liouville operator [i.e., type (i)] are found to be few in comparison to the corresponding isotropic situation. Therefore, few eigenvalues contribute significantly to the spectrum. This is equivalent to stating that an increase of the potential reduces the size of the optimal reduced space, and the computer results (compare in Fig. 3 the rate of convergence between calculations V and I) show that the Lanczos algorithm reproduces this effect, even though we used the spherical harmonics as the initial basis set. In general as long as N is correctly chosen, the value of n_s required for convergence is substantially independent of the choice of the initial basis set.

The previous analysis of the behavior of the Lanczos algorithm for problems involving only the g tensor, can easily be extended to calculations with both g and A tensor. In fact, the introduction of the A tensor is equivalent to substituting each basis element defined by some values of the K and L indices, with a subset representing all the possible transitions (index p and q in Appendix B). In each subset the diffusion operator and the part of the Liouville operator proportional to the g tensor, give a diagonal contribution independent of the transitions, and only the A tensor contributes to the off-diagonal elements. Therefore the extreme eigenvalue effect, since it is related to the diffusion operator, is not really affected by the introduction of these addition transitions. On the other hand the contribution of the different transitions (for each value of the L and K matrices), to the optimal reduced space does depend on the magnitude of the A tensor. Consequently, a reduction of the magnitude of the A tensor decreases n_s.

Calculation VI constitutes a typical slow motional situation for an axial nitroxide probe. The effects of an increased N and of a strong potential are illustrated in

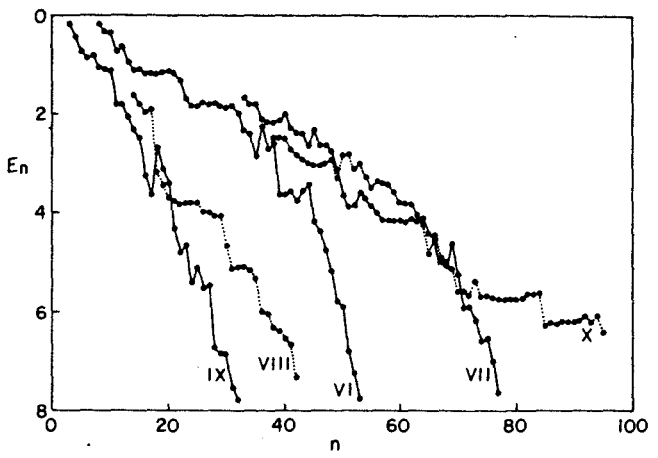

FIG. 4. Behavior of the logarithm of the error: $E_n = -\log_{10}(\Delta_n)$ [Δ_n is defined in Eq. (15)] as a function of the number of steps n in the Lanczos algorithm. (See Table I for the magnetic, diffusion, and truncation parameters.)

calculations VII and IX, respectively. We see from Fig. 4 that the Lanczos algorithm behaves in the same way as the corresponding situations for the simple g tensor. Calculation VIII shows that a decrease of the A tensor leads, as expected, to a more rapid convergence. Finally, calculation X displays the convergence for a typical slow motional spectrum of a nonaxial nitroxide probe.

C. Convergence and efficiency

We now wish to inquire whether we can in an *a priori* fashion estimate n_s for a particular problem. For self-adjoint matrices it is known that for each approximate root λ_j there is an exact λ_j' that satisfies the relation

$$|\lambda_j - \lambda_j'| \leq |\beta_{n+1} C_{nj}| \,, \tag{19}$$

where C is the $n \times n$ transformation matrix that diagonalizes the n-dimensional tridiagonal matrix produced by the Lanczos algorithm.[14,21] Since our matrices are complex symmetric, that relation may not be strictly applicable, and to our knowledge there is no exact criterion for the accuracy of the eigenvalues.

Nevertheless we have found from the computer calculations that in most cases $|\beta_{n+1} C_{nj}|$ constitutes an upper bound for $|\lambda_j - \lambda_j'|$ in the sense that for most eigenvalues relation (19) is satisfied. However, for a few eigenvalues $|\beta_{n+1} C_{nj}|$ is still of the same order as $|\lambda_j - \lambda_j'|$ even though the inequality of relation (19) is violated in a rigorous sense. But in our opinion this relation, even as an approximate form, is of little value in the calculation of ESR spectra. First we mention that to employ such a criterion requires the diagonalization of T_n, but it is more convenient to use the continued fractions relations (14) to obtain the spectrum. Furthermore when we use Eq. (19) to estimate the error in the spectrum [cf. Eq. (15)] using Eq. (13) (and ignoring any error in the estimates of the c_j's) we obtain

$$\Delta_n \leq \sum_j \left| \frac{c_j^2 \beta_{n+1}^2 C_{nj}}{\mathrm{Re}(\lambda_j) + 1/T_2^0} \right| . \tag{20}$$

But from the computer calculations we found that the right-hand side of Eq. (20) often overestimates Δ_n by at least an order of magnitude, and that it is a more slowly decreasing function of n than Δ_n. Therefore this relation is not helpful in finding n_s. In fact as we have already pointed out, the Lanczos algorithm produces an approximation to the optimal reduced space that minimizes the error with respect to the spectral function $I(\omega)$ rather than to the individual eigenvalues. We have no simple relation, between accuracy in the spectrum and accuracy in the eigenvalues.

We have found that an empirical approach is much more useful. In particular, one need only compare the spectrum obtained after the nth step with the previous one [after the $(n-1)$th step]. This procedure has the advantage of interpreting the accuracy directly in terms of the spectral function, and furthermore it can be executed on the tridiagonal form by means of Eq. (14a). This approach is not without risk, because it might happen that the spectrum does not change appreciably for some range of n, even though it is still far from the correct one. It is safe to compare spectra differing by substantially more than one in the number of steps. Finally, with experience from similar calculations one develops a rather good insight into what this difference should be as well as into what n_s should be.

We note that generally the ratio n_s/N decreases with increasing complexity in the description of the ESR problem. In fact in the simplest situation given by the axial g tensor in the anisotropic phase, this ratio is equal to 1, since the matrix is already tridiagonal. On the other hand, the computer results previously described (see in particular calculations I, VI, and X where the MTS was used) show that n_s/N decreases when the A tensor is nonzero and when the tensors are nonaxial. In particular for calculation X, where both these factors contribute, we have $n_s/N \simeq 0.2$.

In the following paragraphs we analyze the use of the Lanczos algorithm from both the point of view of needed storage and of execution time, emphasizing in particular its advantages with respect in the Ruthishauser algorithm.

We first note that the operations in the Lanczos algorithm are always well defined. Instead, in the Rutishauser algorithm the Jacobi rotations are not defined if an element to be eliminated $A_{k,l}$ and its left contiguous one $A_{k,l-1}$ are related by

$$A_{k,l-1} = \pm i A_{k,l} \,. \tag{21}$$

In our experience that never happens in simulations of conventional (unsaturated) ESR spectra, but that need not be the case in other problems. As an example, we mention the simulation of ESR spectra for conditions of saturation.[22]

In the Lanczos algorithm only the storage of two vectors is strictly necessary, while the matrix elements can either be stored or generated when they are needed. The former is preferred if the maximum N for a particular type of problem allows one to store the matrix; (this is the case with a PDP 11/34 minicomputer for

typical calculations of ESR spectra). On the other hand, the second option allows one to solve very large problems in computers that have a limited (or better, large) memory, provided the computation of the matrix elements can be efficiently performed. But, if the first option is to be used, the efficiency of the storage can be considerably increased by considering the sparseness of the matrix, since only the non zero matrix elements are needed. For ESR problems, as described in Appendix B, the suitable parameter to characterize the sparseness is n_B, the average number of matrix elements different from zero for each row counted from the diagonal element. In fact in the limit $L_{max} \gg (I+1)$, n_B tends to a constant, while the ratio between matrix elements different from zero and N^2 tends to zero. We give the limiting value of n_B in two situations:

(i) axial magnetic tensors and $L_{max} \gg (I+1)$:

$$n_B = \delta_\lambda + 8 - 6(I+1)^{-1} ; \tag{22}$$

(ii) nonaxial magnetic tensors, $L_{max} \gg (I+1)$ and $K_{max} \gg (I+1)$:

$$n_B = 2\delta_\lambda + (152I^2 - 26I + 5)(2I+1)^{-2} , \tag{23}$$

where δ_λ is zero if the coefficient λ in the definition [Eq. (B3)] of the pseudopotential is zero, one otherwise. Moreover the number m of elements of n_B that have a real part different from zero is very small [in case (i) $m = 1 + 2\delta_\lambda$, in case (ii) $m = 1 + 4\delta_\lambda$]. Therefore it is convenient to store the real part only if it is different from zero. In this way the needed space in memory, for the matrix elements and the two vectors, is given by $N[(n_B + m)$ real numbers $+ 2(n_B + m)$ integer numbers], where integer numbers are needed to describe the position in the matrix of the matrix elements. An approximate value for N, correct in the limit $L_{max} \gg (I+1)$, is given by the equation

$$N = [(2I+1)/8] \times [(2I+1)K_{max}(2L_{max} - K_{max}) + 4L_{max}(I+1)] . \tag{24}$$

Instead, in the Rutishauser algorithm all the matrix elements in a complex form and within the band structure of the matrix must be stored. Therefore its storage in the limiting situations (i) and (ii) is given by $N(M+1)$ complex numbers, where M is the largest bandwidth of the matrix. In the comparison between the two algorithms from the point of view of storage, the quantities n_B and M must be compared. The maximum bandwidth has the following limit values for the same cases as Eqs. (22) and (23):

$$\text{(i)} \quad M = (2I+1)(2 + I + I\delta_\lambda) + \delta_{I0}(\delta_\lambda - 1) + 1 . \tag{25}$$

$$\text{(ii)} \quad M = \frac{(1+\delta_\lambda)(2I+1)^2 K_{max}}{2} . \tag{26}$$

These relations show clearly an important advantage of the Lanczos algorithm, viz., the bandwidth grows linearly with K_{max} and quadratically with I, while n_B is independent of K_{max} and it reaches a constant limit with increasing I. Moreover the introduction of a mean potential almost doubles the bandwidth, while it implies only the increase of one (or two) for n_B.

The number of multiplications between real numbers in the Lanczos algorithm is approximately $n_s N(2n_B + 21)$. Correspondingly in the Rutishauser algorithm one has about $16N^2M$ multiplications; (this is an upper limit that does not take into account the nullity of elements within the band of the matrix, but this sparseness is progressively destroyed by the Jacobi rotations). Therefore the savings in computation time is given in terms of the ratios n_s/N and $(2n_B + 21)/16M$. We have already discussed this latter ratio, while for the former we recall that, in general, n_s/N decreases with increasing N. Moreover, in minicomputers the efficiency of storage with the Lanczos algorithm implies a further savings in calculation time when the matrix reaches the size in which the Rutishauser algorithm needs a secondary storage device like a disk with consequent increase in calculation time for the large number of reading and writings between core memory and secondary storage device. As an example, calculation X requires about 6 h with the Rutishauser algorithm, while 15 min is sufficient with the Lanczos algorithm.

Another source of savings of computation time is the use of the continued fraction method [see Eqs. (14a)–(14c)] to calculate the spectrum from $\mathbf{T}_n$. Since in this way the number of operations is proportional to n, that is an effort comparable to the calculation of the spectrum by means of Eqs. (13a), (13b) once the eigenvalues λ_j and the components c_j are derived, one saves the execution time for the application of the QR algorithm to $\mathbf{T}_n$. The number of operations in the QR algorithm being proportional to n^2,[6] for large n it could contribute considerably to the total execution time. We remark that this savings in calculation time can be achieved only with the tridiagonal matrix obtained from the Lanczos algorithm, because the Rutishauser algorithm generates, from the starting vector $|v\rangle$, a transformed vector that generally has all its components different from zero.

IV. THE TRUNCATION PROBLEM

ESR problems are in principle described by infinite matrices. Thus the computer calculations require that these matrices be truncated to finite dimension. In order to minimize the execution time as well as to be able to perform the calculation given the limits on the capacity of the available computer, it is important to know how to truncate so as to minimize the size N of the matrix consistent with the results being correct to within the specified accuracy (i.e., the MTS). Moreover, the particular way in which ESR calculations are utilized in routine work emphasizes the importance of this aspect. In fact simulated spectra are compared to the experimental ones in order to derive the values of the principal components of the diffusion tensor and the order parameter λ for the anisotropic phases; (the principal values of the magnetic tensors are usually known from the rigid limit spectra). Therefore for each experimental spectrum one must perform a series of calculations with different values for these parameters. Usually experience suggests a rough estimate of these parameters so that their possible range is limited, and the MTS does not change appreciably for each experimental spectrum. Knowledge of the MTS can considerably speed up this repetitive calculation.

Before analyzing the information given by the Lanczos algorithm, we shall point out what can be derived from the structure of the matrices associated with ESR problems. First of all we emphasize that there is no strict criterion for the MTS; only a comparison between spectra associated with different truncation schemes ultimately assures the convergence of the results. However, it is worthwhile to establish some empirical rules that describe, at least approximately, the dependence of the MTS on the values of the diffusion tensor. (We found that a pseudopotential is of secondary importance in regard to the truncation problem, at least for moderately high values of the parameter λ and for sufficiently slow motion. Therefore the analysis will be limited to the isotropic phase.)

The simplest problem, i.e., the axial g tensor without hyperfine contributions, is useful to characterize the convergence with respect to the index L. In this situation the matrix is already tridiagonal and the error in the spectrum Δ_n, as defined in relation (15) with $n=N$ the dimension of the tridiagonal matrix and $I^R(\omega)$ the correct spectrum (e.g., calculated with a larger value of n), is a rapidly decreasing function of n. More precisely for small n, Δ_n is of the order of the unity, but the error decreases by order(s) of magnitude with increasing n. This behavior is related to the Smoluchowski form of the diffusion operator, since it gives a diagonal contribution that increases as L^2, while the off-diagonal elements derived from the Liouville operator tends to a constant asymptotic value. Therefore, the increase of the size of the matrix, by taking into account high values of the L index, has even more negligible perturbation effect on the spectrum. Our analysis of the MTS for a spectrum correct to within 10^{-4} has yielded the empirical rule

$$L_{\max}^3 = 45\, G_L\,, \tag{27}$$

where the dimensionless parameter G_L describes the slowness of the motion, and it is defined as the ratio between the asymptotic value of the off-diagonal matrix element and the perpendicular component of the diffusion tensor, i.e.,

$$G_L = \tfrac{1}{4}\sqrt{\tfrac{3}{2}}\,\frac{|F_g^{(2,0)}|\omega_0}{D_\perp \bar{g}}\,, \tag{28}$$

and the $F_\mu^{(2,m)}$ are the irreducible tensor components of the μth tensor [cf. Eq. (B1)] where $\bar{g}$ is the mean value of the g tensor. Equation (27) predicts surprisingly well the effect of $D_\perp$ on the MTS.

The MTS for more complicated problems can be derived by means of the rule [Eq. (27)]. First we generalize the analysis to a spin probe in which both the g and A tensors are axial. We have already pointed out in the previous section the similarity in the structure of the matrix between the g tensor problem and the problem with both g and A tensors. Thus Eq. (27) can be extended to this case with a redefined G_L parameter that takes into account the off-diagonal asymptotic contribution of the A tensor

$$G_L = \tfrac{1}{4}\sqrt{\tfrac{3}{2}}\,\frac{|F_g^{(2,0)}|\omega_0/\bar{g} + |F_A^{(2,0)}|\gamma_e I}{D_\perp}\,. \tag{29}$$

We verified the relation (29) for some different situations, always obtaining correct results.

The calculation of $L_{\max}$ does not completely solve the problem of the MTS for this type of problem, since it is still possible to truncate the M and q indices in each subspace. Usually this is not important for the nitroxides, because in these situations only very few basis elements can be eliminated (mostly the doubly forbidden transitions for the higher values of L). On the other hand, this type of truncation becomes very important in dealing with large nuclear spins like the vanadyl complexes ($I=7/2$).

For the most general situation of nonaxial g and A tensors, relation (27) with the parameter G_L defined in relation (29) could be used to calculate $L_{\max}$. For truncating the K index, the same type of considerations for truncating the M and q indices for the axial probe could be applied, i.e., a maximum value for K could be defined for each value of the L index. However we have generally found that $K_{\max}$ is almost independent of L (of course without considering the condition $K \leq L$), and a unique $K_{\max}$ approximates quite well the MTS. An estimate of $K_{\max}$ can be given when $D_\parallel > D_\perp$ (considering the analogy between the tridiagonal form for the axial g tensor and the submatrices defined in the subspace of the basis vectors with the same value of the L index). Also, in this case the off-diagonal elements (or blocks for $I \neq 0$) are determined only by the Liouville operator, and their order of magnitude does not change with the K index, while the diffusion operator gives only a diagonal contribution that grows as K^2. We can also formulate an empirical rule for $K_{\max}$ as

$$K_{\max}^3 = 45\, G_K\,, \tag{30a}$$

where the slowness parameter must now be referred to the $F_\mu^{(2,2)}$ components of the magnetic tensors:

$$G_K = \frac{1}{4}\,\frac{|F_g^{(2,2)}|\omega_0/\bar{g} + |F_A^{(2,2)}|\gamma_e I}{D_\parallel}\,. \tag{30b}$$

In these cases the empirical rules predict the values of $K_{\max}$ and $L_{\max}$ with less certainty than in the axial case [and in some limiting situations they give absurd results (for example when $F_\mu^{(2,0)}=0$ implying $L_{\max}=0$)], since these relations are derived under the strong simplification that the K and L indices can be analyzed independently. Nevertheless, provided these relations are applied with caution, they generally yield an estimate of $L_{\max}$ and $K_{\max}$.

The Lanczos algorithm (L.A.) gives some useful information about the truncation problem that is complementary to the previous empirical rules. For an Hermitian matrix, in the hypothesis that the L.A. chooses the new basis set according to the optimal reduced subspace, and if n_s is the number of steps with which the spectrum is reproduced within a fixed accuracy, then the projection of a particular starting basis element in the n_s dimensional subspace generated by the L.A. gives a direct measure of its contribution to the calculation of the spectrum. For the complex symmetric problems, we define the projections according to the nonmetric form of the scalar product [see Eq. (10)]

$$p_j = \sum_{k=1}^{n_s} \langle x_j | k \rangle^2 \ . \tag{31}$$

This is a simple extension to nonmetric space of the concept of projection that usually is defined in metric space. Therefore the quantities p_j in relation (31) do not have the usual properties of a projection: They are complex quantities and consequently the nullity of p_j does not imply the nullity of all the quantities $\langle x_j | k \rangle$. Nevertheless they constitute, at least from a qualitative point of view, the analog of the "true" projections. In fact if n_s coincides with N, then all the p_j are equal to 1, and if the matrix elements are real, the "true" projections are obtained. Moreover, our interest is to evaluate the contribution of the different starting basis elements to the final spectrum, so we judge as sufficient this qualitative correspondence with the "true" projection. We emphasize that the quantities p_j can be calculated without substantial modification in the computer program (one need only accumulate the quantities $\langle x_j | k \rangle$ each time the L.A. produces a new vector $|k\rangle$).

In order to use correctly the information derived from the projections, one needs to take into account that the L.A. always produces an *approximation* of the optimal reduced space as a consequence of the extreme eigenvalue effect. In the previous section we described how the L.A. tends to reach the higher eigenvalues. The projections p_j for basis elements $|x_j\rangle$ with high values of K and L indices are strongly affected by this behavior and the p_j can have a large value even if the contribution of $|x_j\rangle$ to the spectrum is negligible. Therefore the p_j's are not so informative with respect to the K and L truncation for which the empirical rules [Eqs. (22) and (25)] can be used to supply the needed information. The projections do characterize well the relative contribution of the basis elements that differ only by the indices M and q, for which there is not the extreme eigenvalue effect (cf. Sec. III).

We judge as useful this projection approach to the truncation problem in the calculation of the spectra of a spin probe characterized by a high value of nuclear spin momentum I, since it allows a considerable reduction of the size of the matrix by means of a detailed scheme of truncation for the transitions obtained retaining the basis elements that have $|p_j|$ greater than some value related to the required accuracy. Also, its application in the calculation of ESR spectra of a nitroxide would be very useful when the director for an oriented phase is tilted with respect to the static field. In this situation, the "selection rule" [Eq. (B16)] is no longer satisfied, and the indices M and p must be considered independent of each other with a corresponding increase of the size of the matrix. Also, in this case the projections could give a detailed MTS for the M index.

Lastly, we mention that the projections could be defined so that they are not affected by "the extreme eigenvalue effect." This would be the case if the scalar product $\langle x_j | k \rangle$ in relation (31) is substituted by the scalar product $\langle x_j | y_i \rangle$ (recall $|y_i\rangle$ is an eigenvector of $\mathbf{T}_n$) so that Eq. (31) becomes $p_j' = \sum_{i=1}^{m} \langle x_j | y_i \rangle^2$, where the summation is taken for all the eigenvectors that have a weight greater than the fixed accuracy for the spectrum. We consider this approach strongly limited in practical applications, because it implies:

(i) storage of $\mathbf{Q}_n$ [see Eq. (A1)].

(ii) the use of the QR algorithm with the transformation of all the coefficients of $\mathbf{Q}_n$.

Therefore it is not feasible from both the points of view of storage and calculation time for large size matrices for which the knowledge of the MTS is important.

V. THE LANCZOS ALGORITHM AND FOKKER-PLANCK EQUATIONS

We think that one interesting field of application of the Lanczos algorithm is the calculation of correlation functions from Fokker–Planck equations. In fact, given conditions that we will discuss, this problem is formally similar to the calculation of ESR spectra, and all the results of the previous sections can be applied. In order to examine in detail those formal analogies, we take as a simple example the Fokker–Planck equation for the planar rotator, since it has all the features of the general problem, even though it is described by a very simple equation. Its time evolution is given by the equations[3,23]

$$\frac{\partial P(\gamma, \dot{\gamma}, t)}{\partial t} = -\Gamma P(\gamma, \dot{\gamma}, t) \ , \tag{32a}$$

$$\Gamma = \Gamma_1 + \Gamma_2 \ , \tag{32b}$$

$$\Gamma_1 = \dot{\gamma} \frac{\partial}{\partial \gamma} + \frac{F(\gamma)}{I} \frac{\partial}{\partial \dot{\gamma}} \ , \tag{33a}$$

$$\Gamma_2 = -\beta \frac{kT}{I} \frac{\partial}{\partial \dot{\gamma}} \left(\frac{\partial}{\partial \dot{\gamma}} + \frac{\dot{\gamma}}{IkT} \right) , \tag{33b}$$

where γ is the angle that the rotator makes with the laboratory frame, $\dot{\gamma}$ is the corresponding angular velocity, I is the moment of inertia, and β is the friction coefficient. The force $F(\gamma)$ acting on the rotator is derived from a potential function $V(\gamma)$:

$$F(\gamma) = -\frac{\partial}{\partial \gamma} V(\gamma) \ . \tag{34}$$

Note that the Fokker–Planck operator is separated into two parts: the classical or reversible drift operator Γ_1 and the diffusive or irreversible operator Γ_2. Any correlation function can be written as

$$g(t) = \overline{f_2^*(t) f_1(0)} = \langle f_2 | e^{-\Gamma t} P_{eq} | f_1 \rangle \ , \tag{35}$$

where P_{eq} is the equilibrium distribution function

$$P_{eq} = \exp[-I\dot{\gamma}^2/(2kT) - V(\gamma)/kT]/Z \ , \tag{36}$$

where Z the normalization factor, and the scalar product is defined in the proper Hermitian space for the functions of γ and $\dot{\gamma}$. Defining the symmetrical Fokker–Planck operator $\tilde{\Gamma}$ as

$$\tilde{\Gamma} \equiv P_{eq}^{-1/2} \Gamma P_{eq}^{1/2} \ , \tag{37}$$

we obtain

$$\tilde{\Gamma}_1 = \Gamma_1 \ , \tag{38a}$$

$$\tilde{\Gamma}_2 = -\frac{\beta kT}{I} \left(\frac{\partial}{\partial \dot{\gamma}} - \frac{I\dot{\gamma}}{2kT} \right) \left(\frac{\partial}{\partial \dot{\gamma}} + \frac{I\dot{\gamma}}{2kT} \right) , \tag{38b}$$

and the correlation function can be rewritten as

$$g(t)=\langle f_2 P^{1/2}|e^{-\bar{\Gamma}t}|f_1 P^{1/2}\rangle . \tag{39}$$

Therefore the correlation functions can be calculated once the eigenvalue problem for $\bar{\Gamma}$ is solved.

From the operational form of Γ, it can easily be derived that the matrices associated with the classical evolution operator and the diffusive evolution operator have different kinds of symmetry

$$\bar{\Gamma}_1^{+}=-\bar{\Gamma}_1 , \tag{40a}$$

$$\bar{\Gamma}_2^{+}=\bar{\Gamma}_2 , \tag{40b}$$

where the superscript "+" stands for the adjoint matrix. Therefore the matrix associated with the global time evolution operator will never be self-adjoint. The unique way to solve the problem is to introduce a proper basis set so that the Fokker–Planck operator is represented by a complex symmetric matrix. Moreover, it is always possible to define such a basis set. If we indicate with $\phi_m(\dot{\gamma})\psi_l(\gamma)$ the orthonormal basis set for the problem, a (complex) symmetric matrix representation of $\bar{\Gamma}$ is obtained in two ways:

(i) $\phi_m(\dot{\gamma})=$ real function, $\psi_l(-\gamma)=\psi_l(\gamma)^*$, if the potential obeys the following condition of symmetry: $V(-\gamma)=V(\gamma)$.

(ii) $\phi_m(-\dot{\gamma})=\phi_m(\dot{\gamma})^*$, $\psi_l(\gamma)=$ real function, for any symmetry of the potential.

This can be verified by considering the symmetry properties of each operator (i.e., $\dot{\gamma}$, $\partial/\partial\dot{\gamma}$, etc.) that enters into Eqs. (33a) and (38b). The proper basis functions for case (i) are $\phi_m(\dot{\gamma})=h_m(\dot{\gamma})$, $\psi_l(\gamma)=(2\pi)^{-1/2}e^{il\gamma}$, where $h_m(\dot{\gamma})$ are the eigenfunctions of the one-dimensional quantum-mechanical harmonic oscillator (3, 23) i.e., the Hermite functions. The convenient choice for case (ii) is $\phi_m(\dot{\gamma})=i^m h_m(\dot{\gamma})$, $\psi_l^{s}(\gamma)=[4\pi(1+\delta_{l,0})]^{-1/2}(e^{il\gamma}\pm e^{-il\gamma})$.

The same type of analysis can be applied to more complicated problems like the three-dimensional rotator to obtaining the correct form for the basis set. Once the symmetric matrix associated with $\bar{\Gamma}$ is obtained, the Lanczos algorithm can be applied in order to calculate the correlation function or the corresponding spectral function

$$g(\omega)=\int_0^{\infty} e^{-i\omega t}g(t)dt=\langle f_1 P_{eq}^{1/2}|[i\omega+\bar{\Gamma}]^{-1}|f_2 P_{eq}^{1/2}\rangle . \tag{41}$$

This type of application of the Lanczos algorithm differs from the calculation of ESR spectra in two respects:

(i) two starting vectors are possible: $f_1 P_{eq}^{1/2}$ and $f_2 P_{eq}^{1/2}$.

(ii) in general those vectors have complex components.

The Lanczos algorithm for complex symmetric matrices as described by Eq. (5) can also be applied to a complex starting vector if it is normalized according to Eq. (8), that is,

$$\sum_j \langle x_j|f_i P_{eq}^{1/2}\rangle^2=1 , \quad i=1 \text{ or } 2 . \tag{42}$$

Concerning the first point, the Lanczos algorithm can be generalized so that each time a new basis element is created, its projection on the left-hand vector is calculated. But in our opinion that could render void one of the features that significantly influences the efficiency of the algorithm, viz., the use of a number of steps n much less than the dimension N of the matrix. In fact, it is possible that the left hand vector will continue to have relevant components even as n approaches N. Then, as we have seen (cf. Sec. II), the results will be strongly affected by the loss of orthogonality. In order to best use the algorithm, one needs to reduce the correlation function to a form that does not require the calculation of the transformed left hand vector.

Once $f_2 P_{eq}^{1/2}$ has been chosen as the starting vector, the vectors $|k\rangle$ for $k>1$ produced by the Lanczos algorithm are orthogonal to the left hand vector according to Eqs. (9) and (10), if the functions f_1 and f_2 in the correlation function (35) satisfy the condition

$$\langle l,m|f_2 P_{eq}^{1/2}\rangle=\langle l,m|f_1 P_{eq}^{1/2}\rangle^* , \tag{43}$$

where $|l,m\rangle$ is any element of the initial basis set, e.g., $|l,m\rangle=\phi_m(\dot{\gamma})\psi_l(\gamma)$. Given a function $f(\gamma,\dot{\gamma})$ we define $f^{s}(\gamma,\dot{\gamma})$ as

$$f^{s}(\gamma,\dot{\gamma})=P_{eq}^{-1/2}\sum_{l,m}|l,m\rangle\langle l,m|fP_{eq}^{1/2}\rangle^* . \tag{44}$$

The general correlation function can be reduced to calculations with a single starting vector by means of the relation

$$\overline{f_1(t)^* f_2(0)}=\tfrac{1}{2}\{\overline{[f_1(t)+f_2^{s}(t)]^*[f_2(0)+f_1^{s}(0)]} -\overline{f_2^{s}(t)^* f_2(0)}-\overline{f_1(t)^* f_1^{s}(0)}\} . \tag{45}$$

Each of the three correlation functions on the right-hand side is readily calculated by the Lanczos algorithm. Equation (45) can easily be verified by taking into account the following property which derives from Eq. (39):

$$\overline{f_2^{s*}(t)f_1^{s}(0)}=\overline{f_1(t)^* f_2(0)} . \tag{46}$$

We have previously shown that there are two different complex symmetric matrix representations of the Fokker–Planck operator (32), if the potential is symmetric. We can choose between the two representations in such a way that the computational effort (i.e., the number of times that the Lanczos algorithm is applied) is reduced to a minimum. As an example, if we are interested in correlation functions for real functions of the angular variable, the representation type (ii) is more convenient. In fact the diagonal correlation (i.e., $f_1=f_2$) implies only one diagonalization, since in this case $f^{s}=f$. Moreover the cross correlation function (i.e., $f_1\neq f_2$) requires only one further diagonalization if the two corresponding diagonal correlation functions are known.

Matrices associated with the Fokker–Planck equation (32) will generally have a structure similar to typical matrices for ESR problems, the Liouville operator being substituted by $\bar{\Gamma}_1$ and the diffusion operator by $\bar{\Gamma}_2$ and in particular they are very sparse. Thus in the example of Eq. (33), the size of the matrix is mainly determined by the ratio $\beta/(kT/I)^{1/2}$. The study of the correlation function in the low friction limit, when the Smoluchowski equation is no longer valid, implies di-

agonalization of matrices that grow very rapidly in size. One finds that the ratio between diagonal elements and off-diagonal elements increases only as $m^{1/2}$, with m the index for the basis function for the angular velocity $\phi_m(\hat{\gamma})$, while the ratio in the ESR calculation was proportional to L^2 or K^2.

In conclusion, we think that application of the Lanczos algorithm to the solution of Fokker–Planck equations will be very useful in dealing with problems having a large number of degrees of freedom such as encountered in generalized Fokker–Planck equations in which the effect of the thermal bath is explicitly taken into account.[3]

CONCLUSIONS

(1) The Lanczos algorithm is found to yield very rapid and accurately convergent solutions to the general lineshape problem, and is strongly favored over conventional algorithms.

(2) A conventional algorithm such as that based on the Rutishauser method requires computation times proportional to N^2M (N is the matrix dimension and M is the bandwidth) while the Lanczos algorithm requires times roughly proportional to Nn_sn_B (where n_s is the number of iterative steps and n_B is the average number of nonzero elements in a row). We find $n_s \ll N$ and $n_B \ll M$ especially in the larger problems. This explains its rapidity in execution time.

(3) The required number of iterations n_s can be efficiently determined during the course of a computation (yielding an approximation to the optimal basis set), while N may, with some experience, be truncated to its minimum value (MTS).

(4) Since it is not necessary to store the matrix, problems involving exceedingly large matrices can readily be handled. Our own experience, so far, has been with matrices of N nearly 1000 in complex number (double precision) which could be performed entirely in the core of a minicomputer *even with* matrix storage, so much larger matrices are possible without matrix storage.

(5) The generality of the approach suggests it should prove very useful in a wide variety of problems in magnetic resonance and in stochastic models of molecular dynamics.

ACKNOWLEDGMENTS

We wish to thank Professor C. van Loan for a helpful discussion and Dr. G. P. Zientara and Dr. A. E. Stillman for critically reading the manuscript.

APPENDIX A: ESR SPECTRA IN TERMS OF CONTINUED FRACTIONS

We first demonstrate Eq. (12) for the spectral absorption function. The result of the application of the Lanczos algorithm for $n+1$ steps, as described by the recursive relation [Eq. (7)], can be concisely written in matrix notation[9(b)]:

$$\mathbf{A}\mathbf{Q}_n = \mathbf{Q}_n\mathbf{T}_n + \beta_{n+1}\mathbf{q}_{n+1}\mathbf{e}_n^{tr} , \tag{A1}$$

where $\mathbf{q}_{n+1}$ is the column matrix with the components of $|n+1\rangle$ and $\mathbf{e}_n^{tr}$ is the n-dimensional row matrix defined as $\mathbf{e}_n^{tr} = (0, 0, 0, \cdots, 0, 1)$. The rectangular matrix $\mathbf{Q}_n$ contains the components of the n new basis elements ordered by columns, and it satisfies the normalization condition

$$\mathbf{Q}_n^{tr}\mathbf{Q}_n = \mathbf{1} . \tag{A2}$$

Note that in the general case (i.e., when $n \neq N$) $\mathbf{Q}_n\mathbf{Q}_n^{tr}$ is different from 1. The spectral absorption function Eq. (1) can be written as

$$I(\omega) = (1/\pi)\,\mathrm{Re}\,\{\langle 1|\mathbf{Q}_n^{tr}[(1/T_2^0 + i\omega)\mathbf{1} + \mathbf{A}]^{-1}\mathbf{Q}_n|1\rangle\}, \tag{A3}$$

when the starting vector $|v\rangle$ has only real components and it is normalized (see Appendix B). We indicate with $|1\rangle$ the starting vector $|v\rangle$ represented in the new basis set produced by the Lanczos algorithm, therefore its components are zero except for the first. If $\beta_{n+1} = 0$, we have

$$\mathbf{A}\mathbf{Q}_n = \mathbf{Q}_n\mathbf{T}_n \tag{A4}$$

and Eq. (12) is immediately derived from Eq. (A3) once it has been demonstrated that

$$\mathbf{Q}_n^{tr}\mathbf{A}^{-1}\mathbf{Q}_n = (\mathbf{Q}_n^{tr}\mathbf{A}\mathbf{Q}_n)^{-1} . \tag{A5}$$

This is obviously true if $\mathbf{Q}_n$ is a square matrix, that is, if A is defined in a space with finite dimension N and $n = N$. On the other hand the relation [Eq. (A5)] can easily be verified in the general case, taking into account that Eqs. (A2) and (A4) imply the commutation rule

$$[\mathbf{A}, \mathbf{Q}_n\mathbf{Q}_n^{tr}] = 0 . \tag{A6}$$

The Gauss reduction method,[24] applied to the tridiagonal matrix $[(1/T_2^0 + i\omega)\mathbf{1} + \mathbf{T}_n]$ allows a description of the spectral function in terms of continued fractions. The solution of the linear problem

$$\mathbf{B}|y\rangle = |d\rangle , \tag{A7}$$

where B is a symmetric tridiagonal matrix with dimension n, can be written as

$$\begin{aligned} &w_1 = b_2/a_1 ; \\ &\quad w_j (j = 2, 3, \cdots, n-1) = b_{j+1}/(a_j - b_j w_{j-1}) , \\ &g_1 = d_1/a_1 ; \\ &\quad g_j (j = 2, 3, \cdots, n) = (d_j - b_j g_{j-1}/a_j - b_j w_{j-1}) , \\ &y_n = g_n ; \\ &\quad y_j (j = 1, 2, \cdots, n-1) = g_j - w_j y_{j+1} , \end{aligned} \tag{A8}$$

where y_j and d_j are, respectively, the components of the vectors $|y\rangle$ and $|d\rangle$ and the matrix elements of B are defined as

$$a_j = B_{jj} , \quad b_j = B_{j-1,j} = B_{j,j-1} . \tag{A9}$$

Under the condition that $d_j = \delta_{jn}$, the solution has the simplified form

$$\begin{aligned} &y_j = \prod_{m=j}^{n} (-w_m) , \\ &-w_j b_{j+1} = \frac{-b_{j+1}^2}{a_j +} \; \frac{-b_j^2}{a_{j-1} +} \cdots \frac{-b_2^2}{+ a_1} , \\ &b_{n+1} \equiv -1 , \end{aligned} \tag{A10}$$

where the usual notation for continued fractions is used.[25]

Now applying the previous relations to the tridiagonal matrix defined as

$$a_j = \alpha_{n-j+1} + 1/T_2^0 + i\omega \; ; \quad b_j = \beta_{n-j+2} \, , \tag{A11}$$

where the coefficient α_j and β_j are the matrix elements of T_n, we obtain

$$\langle 1 | \left[\left(\frac{1}{T_2^0} + i\omega \right) \mathbf{1} + \mathbf{T}_n \right]^{-1} | j \rangle = y_{n-j+1} = \prod_{m=1}^{j} \beta_m^{-1} f_m \, , \tag{A12}$$

where $\beta_1 \equiv -1$ and the quantities f_m are defined as

$$f_m = -\beta_m w_{n-m+1} \, , \tag{A13}$$

and therefore they can be written in terms of continued fractions [Eq. (14c)].

By substitution of Eq. (A12) into Eq. (12) for the absorption spectrum and its derivative

$$I'(\omega) = \frac{1}{\pi} \operatorname{Im} \left\{ \sum_{j=1}^{n} \langle 1 | [(1/T_2^0 + i\omega)\mathbf{1} + \mathbf{T}_n]^{-1} | j \rangle^2 \right\} , \tag{A14}$$

Eqs. (14a) and (14b) are immediately derived.

APPENDIX B: MATRIX ELEMENTS IN ESR PROBLEMS

We consider a spin probe with one hyperfine interaction, described by the Hamiltonian in frequency units[1]:

$$\mathcal{H} = \omega_0 S_z + \gamma_e a I_z S_z + \sum_{KM\mu} (-1)^K F_\mu^{(2,-K)} D_{KM}^2(\Omega) A_\mu^{(2,M)} \, , \tag{B1}$$

where the nuclear Zeeman interaction is not taken into account. We assume that the rotational motion is described by the symmetrized Smoluchowski equation[1]:

$$\tilde{\mathbf{\Gamma}} = [\mathbf{J} - (1/2kT)(\mathbf{J}V)]\mathbf{D}[\mathbf{J} + (1/2kT)(\mathbf{J}V)] \, , \tag{B2}$$

where $\mathbf{J}$ is the angular momentum operator, $\mathbf{D}$ is the diffusion tensor, and V is the pseudopotential for oriented phases.

Thereupon the expression for the matrix elements of $(\mathbf{\Gamma} - i\mathfrak{L})$ will be derived without any restriction on the nuclear moment I, but with the following conditions:

(i) The contribution of the nonsecular terms to the spectrum is negligible.

(ii) The tensors $\mathbf{g}$, $\mathbf{A}$, $\mathbf{D}$ are diagonal in the same molecular frame.

(iii) The diffusion tensor is axial with respect to the z direction of the molecular frame.

(iv) The pseudopotential is axial and is given by the relation

$$V = -\lambda k T D_{00}^2(\Omega) \, . \tag{B3}$$

The operator $\mathbf{\Gamma} - i\mathfrak{L}$ is defined in the product space of the Wigner rotation matrices $D_{KM}^L(\Omega)$ and the space of the ESR transitions $|m', m''\rangle$, where m is the eigenvalue of I_z and the eigenstates of the electronic spin are implicit

$$|LKM; m'm''\rangle = \sqrt{\frac{2L+1}{8\pi^2}} \, |D_{KM}^L(\Omega)\rangle |m', m''\rangle \, . \tag{B4}$$

The matrix elements for the diffusion operator are given by the relation

$$\langle L_1 K_1 M_1; m_1' m_1'' | \mathbf{\Gamma} | L_2 K_2 M_2; m_2' m_2'' \rangle$$

$$= \langle m_1' m_1'' | m_2' m_2'' \rangle \delta_{K_1 K_2} \delta_{M_1 M_2} D_\perp \left\{ \left[L_1(L_1+1) + \left(\frac{D_\parallel}{D_\perp} - 1 \right) K_1^2 + \frac{3}{10}\lambda^2 \right] \delta_{L_1 L_2} + N_L(L_1, L_2)(-1)^{M_1+K_1} \left[3\lambda \left(1 - \frac{\lambda}{14} \right) \right. \right.$$

$$\left. \left. \times \begin{pmatrix} L_1 & 2 & L_2 \\ K_1 & 0 & -K_1 \end{pmatrix} \begin{pmatrix} L_1 & 2 & L_2 \\ M_1 & 0 & -M_1 \end{pmatrix} + \frac{18}{35}\lambda^2 \begin{pmatrix} L_1 & 4 & L_2 \\ K_1 & 0 & -K_1 \end{pmatrix} \begin{pmatrix} L_1 & 4 & L_2 \\ M_1 & 0 & -M_1 \end{pmatrix} \right] \right\} \, , \tag{B5}$$

$$N_L(L_1, L_2) = [(2L_1+1)(2L_2+1)]^{1/2} \, ,$$

while for the Liouville operator $\mathfrak{L} = \mathcal{H}^\times$, we obtain

$$\langle L_1 K_1 M_1; m_1' m_2'' | \mathfrak{L} | L_2 K_2 M_2; m_2' m_2'' \rangle = \langle L_1 K_1 M_1; m_1' m_1'' | L_2 K_2 M_2; m_2' m_2'' \rangle \left(\omega_0 + \gamma_e a \frac{m_1' + m_1''}{2} \right)$$

$$+ N_L(L_1, L_2)(-1)^{K_2+M_1} \begin{pmatrix} L_1 & 2 & L_2 \\ K_1 & K_2 - K_1 & -K_2 \end{pmatrix} \begin{pmatrix} L_1 & 2 & L_2 \\ M_1 & M_2 - M_1 & -M_2 \end{pmatrix} \sum_\mu F_\mu^{(2, K_2 - K_1)} \langle m_1' m_1'' | [A_\mu^{(2, M_1 - M_2)}]^\times | m_2' m_2'' \rangle \, , \tag{B6}$$

$$\langle m_1' m_1'' | [A^{(2,M)}]^\times | m_2' m_2'' \rangle = \langle m_2'' | m_1'' \rangle \langle m_1' | A_\mu^{(2,M)} | m_2' \rangle - \langle m_1' | m_2' \rangle \langle m_2'' | A_\mu^{(2,M)} | m_1'' \rangle \, . \tag{B7}$$

The vector of the components is given as

$$\langle LKM; m'm'' | v \rangle = \delta_{K0} \delta_{M0} \delta_{m'm''} (2I+1)^{-1/2} \int d\Omega D_{00}^L(\Omega) P(\Omega)^{1/2} \; ; \quad P(\Omega) = \frac{\exp(-V/kT)}{\int d\Omega \exp(-V/kT)} \, . \tag{B8}$$

The magnetic tensors being diagonal in the molecular frame, the matrix elements have the following symmetry relation:

$$\langle L_1 - K_1 M_1; m_1' m_1'' | \Gamma - i\mathfrak{L} | L_2 - K_2 M_1; m_2' m_2'' \rangle = (-1)^{L_1+L_2} \langle L_1 K_1 M_1; m_1' m_1'' | \Gamma - i\mathfrak{L} | L_2 K_2 M_2; m_2' m_2'' \rangle . \tag{B9}$$

This allows us to reduce the dimension of the problem taking only the positive and even values for the index K corresponding to the redefined basis elements

$$|LKM; m'm''\rangle = [2(1+\delta_{K0})]^{1/2} (|LKM; m'm''\rangle + (-1)^L |L-KM; m'm''\rangle) , \tag{B10}$$

while the relation [Eq. (B5)] remains unchanged and the relation (B6) needs the normalization factor

$$N_K(K_1, K_2) = (1+\delta_{2, K_1+K_2})^{1/2} . \tag{B11}$$

To take into account the symmetry with respect to the index M, we redefine the notation for the transitions in terms of two new indices p and q:

$$p = m' - m'' ; \quad q = m' + m'' . \tag{B12}$$

Therefore the allowed values of the p index are the integer number in the interval $-2I$ to $2I$ while the q index assumes the values $-Q, -Q+2, \cdots, Q$, where $Q = 2I - |p|$. The use of the q index is equivalent to organizing the transitions in terms of allowed transitions ($p=0$), single forbidden transitions ($p=\pm 1$), etc. The quantities in relation (B7) satisfy the symmetry condition

$$\langle p_1 q_1 | [A_\mu^{(2,M)}]^x | p_2 q_2 \rangle = (-1)^M \langle -p_1 q_1 | [A_\mu^{(2,-M)}]^x | -p_2 q_2 \rangle , \tag{B13}$$

that by substitution in Eqs. (B5) and (B6) gives

$$\langle L_1 K_1 - M_1; -p_1 q_1 | \Gamma - i\mathfrak{L} | L_2 K_2 - M_2; -p_2 q_2 \rangle = (-1)^{L_1+L_2+M_1+M_2} \langle L_1 K_1 M_1; p_1 q_1 | \Gamma - i\mathfrak{L} | L_2 K_2 M_2; p_2 q_2 \rangle . \tag{B14}$$

As a consequence the problem can be further reduced, redefining the basis set as

$$|LKM; pq\rangle = [2(1+\delta_{0M}\delta_{0p})]^{-1/2} \times (|LKM; pq\rangle + (-1)^{L+M} |LK-M; -pq\rangle) , \tag{B15}$$

where the index M is now positive.

The quantities in relation (B13) have the "selection rule"

$$\langle p_1 q_1 | [A_\mu^{(2,M)}]^x | p_2 q_2 \rangle = 0 , \quad \text{for } p_1 \neq p_2 + M . \tag{B16}$$

That implies a further factorization of the problem and the needed basis elements are

$$|LKM; q\rangle \equiv |LKM; Mq\rangle , \quad M = 0, 1, \cdots, \mathrm{Min}\{L, 2I\} , \quad q = -Q, -Q+2, \cdots, Q , \tag{B17}$$

where $Q = 2I - M$. In this new representation the relation (B5) remains unchanged while the Liouville operator has the following expression for the matrix elements:

$$\langle L_1 K_1 M_1; q_1 | \mathbf{L} | L_2 K_2 M_2; q_2 \rangle = \langle L_1 K_1 M_1; q_1 | L_2 K_2 M_2; q_2 \rangle \left(\omega_0 + \frac{\gamma_e a q_1}{2}\right) + N_L(L_1, L_2) N_K(K_1, K_2) N_M(M_1, M_2) (-1)^{M_1} \times \begin{pmatrix} L_1 & 2 & L_2 \\ K_1 & K_2 - K_1 & -K_2 \end{pmatrix} \begin{pmatrix} L_1 & 2 & L_2 \\ M_1 & M_2 - M_1 & -M_2 \end{pmatrix} \sum_\mu F_\mu^{(2, K_2-K_1)} G_\mu^{(M_1, q_1; M_2, q_2)} , \tag{B18}$$

$$N_M(M_1, M_2) = (1+\delta_{1, M_1+M_2})^{1/2} , \quad G_g(M_1, q_1; M_2, q_2) = \delta_{q_1 q_2} \delta_{M_1 M_2} \sqrt{\tfrac{2}{3}} \omega_0 / \bar{g} ,$$

$$G_A(M_1, q_1; M_2, q_2) = \frac{\delta_{M_1 M_2} \delta_{q_1 q_1} q_1 \gamma_e}{\sqrt{6}} + \delta_{1, |M_1 - M_2|} \delta_{q_1, q_2 \pm 1} \gamma_e (M_2 - M_1) \sqrt{I(I+1) - \tfrac{1}{2}[q_1 \pm M_1(M_1 - M_2)]} \sqrt{\tfrac{1}{2}[q_2 \pm M_2(M_1 - M_2)]} .$$

We remark that the matrix associated with $\Gamma - i\mathfrak{L}$ is complex symmetric, both Γ and $\mathfrak{L}$ being real symmetric.

[1] (a) J. H. Freed, G. V. Bruno, and C. F. Polnaszek, J. Phys. Chem. 75, 3385 (1971); J. Chem. Phys. 55, 5270 (1971); B. Yoon, J. M. Deutch, and J. H. Freed, *ibid.* 62, 4687 (1975). (b) C. F. Polnaszek, G. V. Bruno, and J. H. Freed, *ibid.* 58, 3185 (1973).

[2] S. A. Goldman, G. V. Bruno, C. F. Polnaszek, and J. H. Freed, J. Chem. Phys. 56, 716 (1972); J. S. Hwang, R. P. Mason, L. P. Hwang, and J. H. Freed, J. Phys. Chem. 79, 489 (1975); C. F. Polnaszek and J. H. Freed, *ibid.* 79, 2283 (1975); R. F. Campbell and J. H. Freed, *ibid.* 84, 2668 (1980); E. Meirovitch and J. H. Freed, *ibid.* 84, 2459 (1980); M. Shiotani, G. Moro, and J. H. Freed, J. Chem. Phys. 74, 15 (1981).

[3] (a) A. E. Stillman and J. H. Freed, J. Chem. Phys. 72, 550 (1980); (b) A. E. Stillman and J. H. Freed (to be published).

[4] (a) J. H. Freed, in *Spin Labelling: Theory and Applications*, edited by L. J. Berliner (Academic, New York, 1976); E. Meirovitch and J. H. Freed, J. Phys. Chem. 84, 3281, 3295 (1980); (b) R. F. Campbell, E. Meirovitch, and J. H. Freed, J. Chem. Phys. 83, 525 (1979); E. Meirovitch and J. H. Freed, Chem. Phys. Lett. 64, 311 (1979); O. Pschorn and H. W. Spiess, J. Mag. Reson. 39, 217 (1980).

[5] H. Rutishauser, in Proceedings of the American Mathematics Society Symposium on Applied Mathematics, 1963, Vol. 15, p. 219.

[6] R. G. Gordon and T. Messenger, in *Electron-Spin Relaxation in Liquids*, edited by L. T. Muus and P. W. Atkins (Plenum, New York, 1972).

[7] R. F. Hausman, S. D. Bloom, and C. F. Bender, Chem. Phys. Lett. 32, 483 (1975); H. Nissimov, Phys. Lett. 46 B, 1 (1973); M. C. M. O'Brien and S. N. Evangelou, J. Phys. C 13, 611 (1980); J. M. F. Gunn, *ibid.* 13, 3755 (1980); R. Haydock, V. Heine, and M. J. Kelly, *ibid.* 8, 2591 (1975); J. Stein and U. Krey, Z. Phys. B 34, 287 (1979); 37, 13 (1980); R. Haydock, Solid State Phys. 35, 216 (1980); M. J. Kelly, *ibid.* 35, 296 (1980).

[8]S. Alexander, A. Baram, and Z. Luz, J. Chem. Phys. 61, 992 (1974); A. Baram, *ibid.* 71, 2503 (1979). They give an expression equivalent to the Lanczos algorithm but provide few details.
[9](a) C. Lanczos, J. Res. Natn. Bur. Stand. 45, 255 (1950); 49, 33 (1952); (b) B. N. Parlett, *The Symmetric Eigenvalue Problem* (Prentice Hall, Englewood Cliffs, N. J., 1980).
[10]G. Moro and J. H. Freed, J. Phys. Chem. 84, 2837 (1980).
[11]Yu. V. Vorobyev, *Method of Moments in Applied Mathematics* (Gordon and Breach, New York, 1965).
[12]D. Masson, in *The Padé Approximant in Theoretical Physics*, edited by G. A. Baker and J. L. Gammel (Academic, New York, 1970).
[13]G. A. Baker, *Essentials of Padé Approximants* (Academic, New York, 1975).
[14]W. Kahan and B. N. Parlett, in *Sparse Matrix Computations*, edited by J. Bunch and D. Rose (Academic, New York, 1976).
[15]C. C. Paige, J. Inst. Maths. Its Appl. 10, 373 (1972); *ibid.* 18, 341 (1976).
[16]J. J. Dongarra, C. B. Moler, J. R. Bunch, and G. W. Stewart, *LINPACK User's Guide* (SIAM, Philadelphia, 1979).
[17]G. Moro, *The Subroutine TRIDG* (unpublished report).
[18]G. Van Loan, in *Numerical Algorithms in Chemistry: Algebraic Methods* (NRCC, Berkeley, 1978).
[19]P. J. Brussdard and H. A. Tolhoek, Physica 23, 955 (1957).
[20]P. L. Nordio and V. Segre, J. Magn. Reson. 27, 465 (1977).
[21]L. Fox, *Introduction to Numerical Linear Algebra* (Oxford University, New York, 1965).
[22]S. A. Goldman, G. V. Bruno, and J. H. Freed, J. Chem. Phys. 59, 3071 (1973).
[23]G. V. Bruno and J. H. Freed, J. Phys. Chem. 78, 395 (1974).
[24]F. B. Hildebrand, *Methods of Applied Mathematics* (McGraw-Hill, New York, 1956).
[25]H. S. Wall, *Analytic Theory of Continued Fractions* (Van Nostrand, Princeton, 1948).